

# Synthesis of TiO<sub>2</sub> nanotubes by hydrothermal method applicable to dye sensitized solar cells

MAHDI MALEKSHAHI BYRANVAND\*, ALI NEMATI KHARAT

School of Chemistry, University College of Science, University of Tehran, Tehran, Iran

TiO<sub>2</sub> nanotubes (NTs) were synthesized using a simple template-free sol-gel and hydrothermal methods. The TiO<sub>2</sub> NTs applied to make photoelectrode for dye sensitized solar cells (DSSCs). The prepared samples were characterized by X-ray powder diffraction (XRD), transmission electron microscopy (TEM), and scanning electron microscopy (SEM). Formation of highly crystalline anatase TiO<sub>2</sub> NTs was confirmed. The prepared photoelectrode with TiO<sub>2</sub> NTs was then employed to fabricate DSSCs. The TiO<sub>2</sub> NTs photoelectrode composite has better photoelectric properties than same mesoporous electrode. The solar energy conversion efficiencies ( $\eta$ ) for fabricated cell with prepared TiO<sub>2</sub> NTs were about 2.53%.

(Received May 13, 2014; accepted January 21, 2015)

**Keywords:** TiO<sub>2</sub> NTs, TiO<sub>2</sub> mesoporous, DSSCs, Hydrothermal method

## 1. Introduction

Dye-sensitized solar cells (DSSCs) have attracted much attention for the last more than a decade since they were developed by Gratzel in 1980s [1-4] because of their low-cost, environment friendliness and high conversion efficiency of solar energy into electrical energy compared to silicon cells [5-7]. A typical DSSC consists of a layer of nanostructured TiO<sub>2</sub> covered with sensitizing dye as photoelectrode and electrolyte containing a redox mediator (I<sup>-</sup>/I<sub>3</sub><sup>-</sup>) placed between photoelectrode and counter electrode (Fig. 1) [8]. Significant progress has been made recently to enhance the efficiency, including novel sensitized dyes, electrolytes, and photoanodes (nanocrystalline metal oxide films) [9].

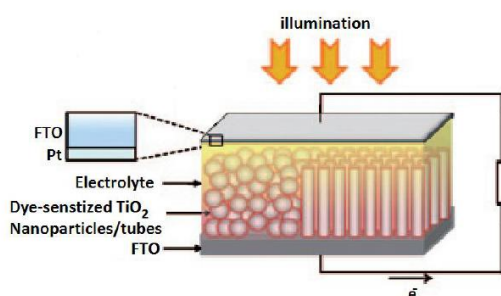


Fig. 1. Schematic diagram of the DSSC with nanostructured TiO<sub>2</sub>.

Bulk TiO<sub>2</sub> is known to be a very useful non-toxic, environmentally friendly, corrosion-resistant material: it is frequently used in paint, white pigments, and sun-blockers. TiO<sub>2</sub> in all its crystal forms is a wide-band gap semiconductor ( $E_g \sim 3$  eV) with suitable band-edge positions that enable its use in DSSCs [3, 10-12]. The

morphology of TiO<sub>2</sub> can be widely tuned to achieve the best efficiency. Using the very high surface area, which is provided by the nanocrystalline particles of TiO<sub>2</sub>, DSSCs allowed for an adsorption of a sufficiently large number of dye molecules for efficient light harvesting [13, 14].

The decrease of electron diffusion coefficient in the nanocrystalline particles of TiO<sub>2</sub> can be a consequence of the presence of electron traps that occur in the grain boundaries at the contacts between these nanoparticles. Thus, the use of TiO<sub>2</sub> in the form of nanorods, nanowires and especially nanotubes (NTs) may be an interesting approach to improve electron transport through the film and may allow for a much higher control of the chemical or physical behavior. By diminishing dimensions to the nanoscale, not only the specific surface area increases significantly but also the electronic properties may change considerably. The TiO<sub>2</sub> NTs were usually prepared by electrochemical approach [15], layer-by-layer assembly [8], template synthesis, sol-gel method [12], etc. These methods require either suitable templates or special equipments and technologies, which suffers from either low yields or the high cost. In current investigation, the sol-gel synthesis of mesoporous TiO<sub>2</sub> and subsequently one-dimensional TiO<sub>2</sub> NTs synthesis by hydrothermal method and their utilization in DSSC are discussed.

## 2. Experimental

### 2.1. Synthesis of TiO<sub>2</sub> mesoporous

TiO<sub>2</sub> mesoporous was prepared by a sol-gel process followed by growth under hydrothermal condition [12]. A volume 62.5 ml of distilled water and 20 ml of glacial acetic acid (Merck) were mixed into a 500 ml round bottom flask under ice bath. A mixture of 2.5 ml of 2-propanol (Merck) and 9.25 ml of titanium (IV) butoxide

(Merck) was then dropped slowly to the acetic acid solution over a 30-40 min period under vigorous stirring. Then, transparent colloid was under reflux condition for 8 h under vigorous stirring in 80 °C hot water bath. The resulting gel was autoclaved at 230 °C for 12 h and slowly cooled down to room temperature. Resulting solution was filtered after centrifuging (SIGMA model) under 7800 rpm for 10 min, this process was repeated three times until the precipitation of titanium dioxide was completed. The precipitate was then washed several times with distilled water. Finally the product was dried at 100 °C for 24 h.

## 2.2. Synthesis of one-dimensional TiO<sub>2</sub> NTs

In a typical synthesis [16], 5 g TiO<sub>2</sub> mesoporous powders prepared by sol-gel method was placed into a Teflon-lined autoclave of 500 ml capacity. Then, the autoclave was filled with 80 ml NaOH (10M) (Merck) aqueous solution, sealed into a stainless tank and maintained at 140 °C for 16 h. Prepared slurry was removed from vessel (using deionized (D.I.) water) and then neutralized and ion-exchanged by 0.1 M HCl (in D.I. water) to reduce the pH level up to 1.0 slowly and then washed three times with D.I. water through centrifugation process. After washing, the slurry was dried in freeze and vacuum-dryer under 50 °C for 1 day. To convert from amorphous phase to anatase phase, prepared powder was treated under high temperature (500 °C for 30 min).

## 2.3. TiO<sub>2</sub> mesoporous and nanotube paste preparation

The 2 g of TiO<sub>2</sub> powder was transferred into a porcelain mortar. Then 2 ml D.I. water and 3 ml acetyl acetone (Merck) were added and mixed well with the TiO<sub>2</sub> powder by grinding. Another 3 ml of D.I. water was added and the mixture was ground until the particles were dispersed well by the high shear forces in the viscous past. Additional 8 ml D.I. water was added slowly in 0.5 ml increment to dilute the viscous paste under continued grinding. Finally, a few drops (0.2 ml) of surfactant (Triton X-100, Aldrich) were added to the TiO<sub>2</sub> dispersion.

## 2.4. DSSCs fabrication

In a typical fabrication procedure, FTO substrates (TCO 10-10, 2.5 cm × 2.5 cm, solaronix) with surface resistivity ~20 Ω/sq were sonicated with acetone and ethanol at 60 °C for 1 h. The prepared TiO<sub>2</sub> paste (mesoporous and nanotube) was then coated onto FTO conductive glass using the screen printing and sintered in 450 °C for 30 minutes. The photoelectrode were sensitized by immersing them in 0.3 mM N719 dye (Ruthenium 535-bisTBA, solaronix) in anhydrous ethanol solution for 24 h. Electrodeposition was carried out using an aqueous solution of 16 ml of dinitroamine platinum (II), 100 g of

sodium carbonate and 40 g of sodium acetate in 1000 ml of distilled water. Pt electrode (counter electrode) was prepared by current density of 0.2 A/dm<sup>2</sup> with the 10 s on-time and 10 s off time at room temperature. The dye-covered mesoporous and NTs TiO<sub>2</sub> film and the counter electrodes were assembled into sealed sandwich-type cells applying one drop of electrolyte (MPN-100, solaronix) and sealing with Amosil 4 (solaronix).

## 2.5. Characterization

The crystalline structure of the samples was evaluated by X-ray diffraction (XRD, RIGAKURINT2100). The nanostructure of the prepared materials was analyzed by scanning electron microscopy (SEM, JEOL JSM-6500FE) and transmission electron microscopy (TEM, JEOL JEM-200CX). The photocurrent-voltage characteristics were measured with a potentiostat (chi660a) under illumination. A 1000 W Xenon lamp was employed as the light source in conjunction with an IRA-25S filter (Schott, USA) to get rid of the UV light. The light intensity corresponding to AM 1.5 (100 mW/cm<sup>2</sup>) was calibrated using a standard silicon solar cell.

## 3. Results and discussion

### 3.1. Characterization of nanostructured TiO<sub>2</sub>

The crystal structure is confirmed by the X-ray diffraction (XRD) analysis. Fig. 2a, b shows the XRD pattern of the mesoporous and nanotube TiO<sub>2</sub> synthesized sample respectively. All the relatively sharp peaks could be indexed as anatase TiO<sub>2</sub> with crystalline cell constants  $a = 3.783\text{Å}$  and  $c = 9.51\text{Å}$ , which indicated they obtained TiO<sub>2</sub> had relatively high crystallinity, and these peaks are basically in agreement with the reported values Joint Committee on Powder Diffraction Standards (JCPDS) card No. 04-0477. Considering the X-Ray diffraction pattern the mean particle diameter can be calculated from Scherrer equation (1):

$$T = \frac{K\lambda}{\beta \cos \theta} \quad (1)$$

Where K is the shape factor has a typical value of about 0.9,  $\lambda$  is the x-ray wavelength, typically 1.54 Å,  $\beta$  is the line broadening at half the maximum intensity (FWHM) in radians,  $\theta$  is the Bragg angle and T is the mean size of the ordered (crystalline) domains. Using equation (1) the mesoporous TiO<sub>2</sub> size was estimated to be about 25-27 nm.

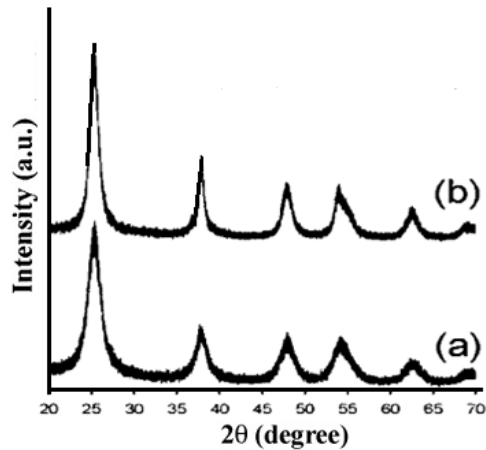


Fig. 2. X-ray diffraction pattern of the as-synthesized (a) mesoporous and (b) nanotube TiO<sub>2</sub> anatase.

Scanning electron microscopy (SEM) and transmission electron microscopy (TEM) images of the synthesized sample reconfirming the nanostructure of prepared powder by sol-gel method are shown in Fig. 3 (a, b and c) that correspond with XRD pattern of the samples. High crystallinity of synthesized TiO<sub>2</sub> with clear lattice fringes is confirmed by HRTEM images of the synthesized sample. The lattice fringes of the nanoparticles appearing in the image ( $d = 0.35$  nm) also allowed for the identification of the anatase phase (Fig. 3d).

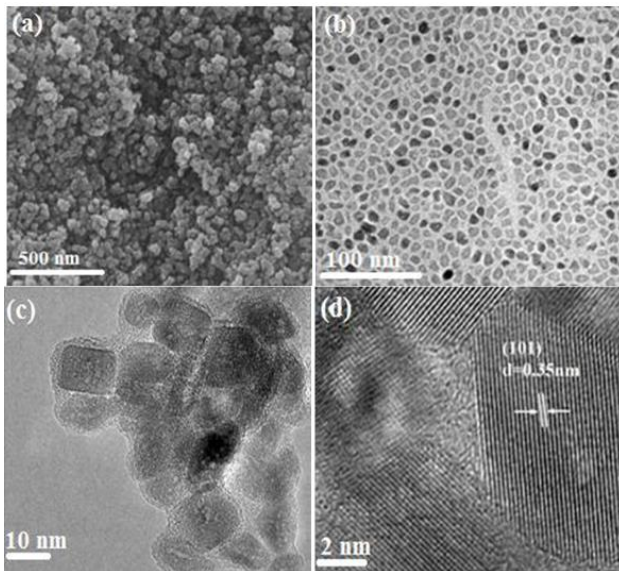


Fig. 3. (a) SEM, (b-d) TEM images of the synthesized mesoporous anatase TiO<sub>2</sub> nanopowders.

The TiO<sub>2</sub> NTs were obtained after hydrothermal synthesis, showing very clear morphology and well-defined structure (Fig. 4a). TEM images (Fig. 4b) demonstrate that NTs grow extensively with the length of several hundred nanometers with quite clean and smooth tubular surfaces. No TiO<sub>2</sub> particles exist around the NTs, proving high yield conversion of TiO<sub>2</sub> synthesized powder to NTs under experiment conditions.

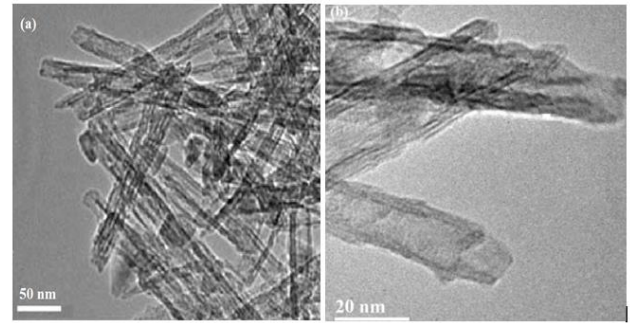


Fig. 4. (a, b) TEM image of TiO<sub>2</sub> NTs were obtained after hydrothermal synthesis.

### 3.2. Characterization of fabricated DSSCs

The fill factor for DSSC was calculated from equation (2) where  $P_{\max}$  is the maximum electrical power obtained;  $I_{SC}$  and  $V_{OC}$  are the short-circuit current density and open-circuit voltage, respectively.

$$FF = \frac{P_{\max}}{I_{SC} \times V_{OC}} \quad (2)$$

The conversion efficiency of the DSSC is obtained from equation 3. Where  $I$  is the intensity of incident light;  $A$  is the active area illuminated by halogen lamp.

$$\eta = \frac{I_{SC} \times V_{OC} \times FF}{I \times A} \quad (3)$$

The photocurrent-voltage curve for the fabricated solar cells using synthesized nanostructured TiO<sub>2</sub> operated with platinum counter electrode is shown in Fig. 5.

The values of  $V_{OC}$ ,  $J_{SC}$ , FF and cell efficiency ( $\eta$ ) for the fabricated cells with different photoelectrode of active area  $1\text{cm}^2$  illuminated by a halogen lamp with an incident light of  $100\text{ W/cm}^2$  is shown in Table 1 and Fig. 5. As seen in table the FF values for fabricated cells with different photoelectrode approximately are equal, and types of nanostructured used in this work have no impressive effect on FF. The use of TiO<sub>2</sub> NTs photoelectrode facilitates the electron transfer process to regenerate the electrolyte in the cell explaining the higher  $J_{SC}$  and  $\eta$  values over the TiO<sub>2</sub> mesoporous photoelectrode.

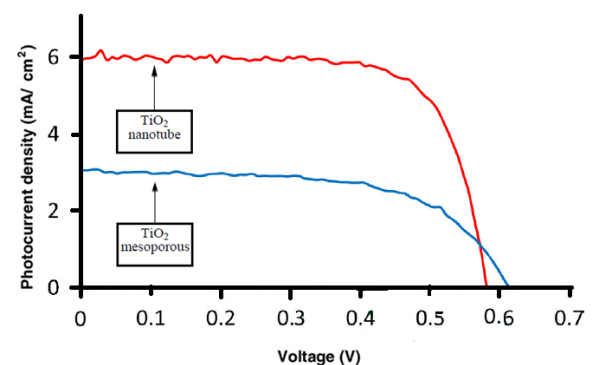


Fig. 5. Photocurrent-voltage characteristics for DSSCs under illumination of  $100\text{ mWcm}^{-2}$  (AM 1.5).

Table 1. Photovoltaic performance for fabricated cells.

Fabricated DSSC	V <sub>OC</sub> (V)	J <sub>SC</sub> (mA/cm <sup>2</sup> )	FF %	η %
TiO <sub>2</sub> mesoporous	0.611	3.05	60	1.13
TiO <sub>2</sub> NTs	0.582	5.97	73	2.53

#### 4. Conclusion

Nanocrystalline TiO<sub>2</sub> mesoporous have been successfully synthesized by sol-gel method. Subsequent fine purity structures of one-dimensional TiO<sub>2</sub> NTs were successfully produced with the use of as synthesized TiO<sub>2</sub> mesoporous via hydrothermal method and then applied in DSSCs. The properties of DSSC based on TiO<sub>2</sub> NTs films were studied. For the TiO<sub>2</sub> NTs film, the conversion efficiency showed the best result. The photovoltaic response could be attributed to the structural and electronic properties of the NTs, which demonstrate a better performance than the other nanostructures investigated.

#### Acknowledgment

The authors are grateful for a grant from university of tehran.

#### References

- [1] B. O'Regan, M. Gratzel, *Nature*, **353**, 737 (1991).
- [2] L. M. Peter, *The Journal of Physical Chemistry C*, **111**, 6601 (2007).
- [3] Z. Sun, J. H. Kim, T. Liao, Y. Zhao, F. Bijarbooneh, V. Malgras, S. X. Dou, *CrystEngComm*, **14**, 5472 (2012).
- [4] A. Hagfeldt, G. Boschloo, L. Sun, L. Kloo, H. Pettersson, *Chem. Rev.*, **110**, 6595 (2010).
- [5] R. Simoes, V. F. Neto, J. C. Mendes, L. Pereira, *Electro/Information Technology (EIT)*, 2013 IEEE International Conference on, 1 (2013).
- [6] M. H. Oliveira Jr, D. S. Silva, A. D. S. Côrtes, M. A. B. Namani, F. C. Marques, *Diamond and Related Materials*, **18**, 1028 (2009).
- [7] M. D. Brown, T. Suteewong, R. S. Kumar, V. D'Innocenzo, A. Petrozza, M. M. Lee, U. Wiesner, H. J. Snaith, *Nano Lett.*, **11**, 438 (2011).
- [8] M. M. Byranvand, K. Ali Nemati, B. Mohammad Hossein, *Nano-Micro Letters*, **4**, 253 (2012).
- [9] M. M. Byranvand, M. H. Bazargan, A. Nemati Kharat, L. Fatholahi, *Optoelectron. Adv. Materials – Rapid Comm.*, **5**, 360 (2011).
- [10] M. Guo, K. Xie, J. Lin, Z. Yong, C. T. Yip, L. Zhou, Y. Wang, H. Huang, *Energy & Environmental Science*, **5**, 9881 (2012).
- [11] A. Thorne, A. Kruth, D. Tunstall, J.T.S. Irvine, W. Zhou, *The Journal of Physical Chemistry B*, **109**, 5439 (2005).
- [12] M. H. Bazargan, M. M. Byranvand, A. N. Kharat, *International Journal of Materials Research*, **103**, 347 (2012).
- [13] S. Mathew, A. Yella, P. Gao, R. Humphry-Baker, F. E. Curchod, N. Ashari-Astani, I. Tavernelli, U. Rothlisberger, K. Nazeeruddin, M. Grätzel, *Nat Chem*, **6**, 242 (2014).
- [14] S. Chang, Q. Li, X. Xiao, K.Y. Wong, T. Chen, *Energy & Environmental Science*, **5**, 9444 (2012).
- [15] N. Liu, H. Mirabolghasemi, K. Lee, S. P. Albu, A. Tighineanu, M. Altomare, P. Schmuki, *Faraday Discuss.*, (2013).
- [16] M. Malekshahi Byranvand, A. Nemati Kharat, L. Fatholahi, Z. Malekshahi Beiranvand, *Optoelectron. Adv. Mater. Rapid Comm.* **7**, 961 (2013).

\*Corresponding author: Mahdi.malekshahi@gmail.com